INDOOR USER ZONING AND TRACKING IN PASSIVE INFRARED SENSING SYSTEMS

Gianluca Monaci, Ashish Pandharipande

Philips Research, 5656AE Eindhoven, The Netherlands
Email: {gianluca.monaci, ashish.p}@philips.com

ABSTRACT

We consider the problem of indoor user zoning - identifying regions occupied by users in a room, and tracking using a grid of passive infrared (PIR) sensors. Under the proposed scheme, quantized levels of analog signal output from pairs of PIR sensors are used to determine an occupied zone. Viterbi-based tracking is employed to further improve the robustness of zoning and track the zones traversed by a user. Experiment results are presented to validate the efficacy of the proposed method for one-dimensional user zoning and tracking.

Index Terms— User zoning, PIR sensing system, Viterbi tracking.

1. INTRODUCTION

Indoor user zoning, i.e. determining occupied regions within rooms in a building, and tracking is of interest in the control of lighting and HVAC systems and building management systems [1], [10]. We consider indoor user zoning and tracking using a passive infrared (PIR) sensing system. The system under consideration comprises of PIR sensors spaced apart in a grid at the ceiling of a room. The processed output of the PIR sensors is collected at a fusion center where occupied zones are determined and user movement is tracked.

A PIR sensor provides a low-cost, low-complexity solution for detecting user presence. A grid of PIR sensors is thus attractive for spatially fine-grained occupancy determination. Most of the existing approaches to user localization consider the binary data output (e.g. presence / no-presence signal) from individual PIR sensors. As a result, the uncertainty of the localization is limited by the size of the sensors' detection area. Slightly finer localization can be obtained by exploiting the overlap of detection areas of neighboring sensors. For a binary sensor network, a particle filtering approach to single target tracking was considered in [4]. A tracking algorithm robust to sensor failures was developed in [5]. Simple coarse localization based on knowledge of spatial topology of a binary sensing system was considered in [6]. In [12], conditions under which multiple targets can be counted were presented under a binary sensing model.

This work was supported by the CATRENE project CA502, *Solutions for Energy Efficient Lighting* (SEEL).

There is limited literature on using the analog, unprocessed PIR sensor output in order to better understand user movements. An analytical model was developed in [8] for the PIR analog output and target tracking algorithms based on extended Kalman filtering were proposed. In [14], features in the PIR analog signal were exploited to extract information on people movements, under a specific configuration with pairs of PIR sensors facing each other. These works show that richer information can be potentially extracted from the raw data, than just presence.

Motivated by the approaches in [8] and [14], we consider processing the analog signal output from PIR sensors. Our proposed method is motivated by the following observations related to the PIR analog output signals and detection regions: (i) the sign of the PIR trigger output voltage is indicative of the direction of user motion with respect to the sensor, and (ii) when the detection regions of different PIR sensors partly overlap, it is possible to associate their corresponding signal levels to spatial zones. Output signals from multiple PIR signals can thus be used to *encode* spatial zones.

In our proposed approach, each PIR sensor quantizes its output signal using two threshold values and sends the result to the fusion center. This ensures low communication overhead between the PIR sensors and the fusion center. The transmitted results from a pair of PIR sensors with partially overlapping detection regions are then used to encode spatial zones, based on which occupancy in a zone is determined. The proposed method allows a much finer localization than that achievable using only the binary output of the PIR sensors. Such user zoning, in practice, may be erroneous, e.g. due to errors in the thresholding and quantization step. To deal with this, we consider a Markov model to characterize human movement, or in other words the transition of spatial zone occupancy. Viterbi-based tracking [11], [13] is then employed to determine zone occupancy and track a user based on the maximized probability state path.

2. PIR SENSING SYSTEM AND SENSOR SIGNAL DESCRIPTION

We consider a PIR sensing system with multiple PIR sensors located on a grid with uniform spacing along the ceiling. This arrangement is typical for lighting systems where the sensor

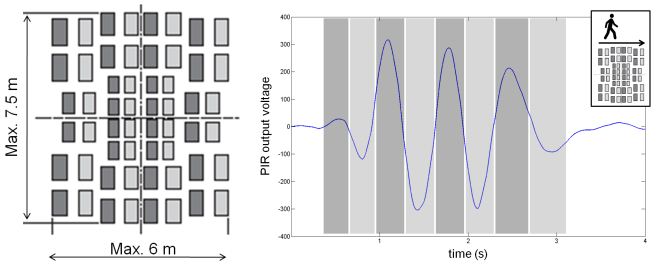

(a) (b)

Fig. 1. (a) Detection region of the Murata IRS A330ST02 sensor with IML-0669 lens, and (b) output voltage of a PIR sensor.

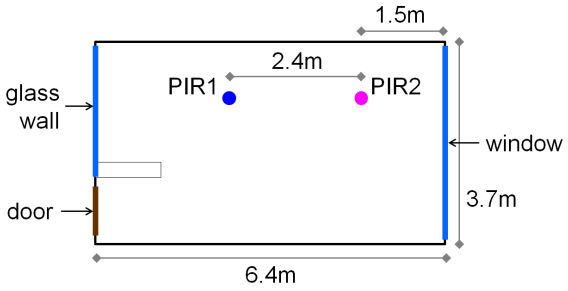

Fig. 2. Layout of experimental office room.

is embedded in the luminaire. We assume that the inter-sensor distance is known and the PIR sensors have overlapping detection regions. The output of an individual PIR sensor is connected to a fusion center, or central controller, where the occupied zones are determined. Based on this information, illumination from the lighting system may be adapted [10].

The core of a PIR sensor is a pyroelectric crystal that generates a voltage change in response to change in temperature [3]. A change in temperature may occur due to infrared radiation from human body as a user comes within the sensing coverage area. Commercial PIR sensors typically include two sensitive elements wired as opposite inputs to a differential amplifier to cancel changes in the ambient temperature [7]. The sensing coverage area of the sensor is usually shaped by an array of Fresnel lenses, which can be molded from infrared transmitting plastic materials. A lenses array creates multiple cones of views, allowing the PIR sensor to be sensitive to human movement within its coverage area. As an example, Figure 1(a) shows the detection region of a Murata IRS-A330ST02-R2 sensor with a Murata IML-0669 lens for an installed height of 2.5 m. We assume that the geometry of this region for the sensor-lens module is available (from the manufacturer data sheet [7]).

The detection region in Figure 1(a) shows the coverage area, with the dark and light gray cells representing projections on the two pyroelectric elements. That is, infrared radiation from a dark gray cell in Figure 1(a) is projected by the lens on one pyroelectric element, while the radiation coming from the light gray cells is projected on the second pyroelectric element. The signals generated by the two elements are subtracted to generate the output differential signal. This sensor-lens module is mainly sensitive to changes along the direction of its minor axis (left-right in Figure 1(a)). When a person moves across the sensing area, the two elements sense the temperature change with a time delay, causing alternate positive and negative peaks. Figure 1(b) shows the output voltage signal of a PIR sensor when a person walks below it along its minor axis. Positive and negative peaks appear one after the other and their positions relate to the location of the person in the coverage area. For a given movement, the signal amplitude is related to the proximity of the person to the sensor: peaks are larger when a user is close to the sensor than when further away.

3. PROPOSED USER ZONING AND TRACKING SCHEME

We shall illustrate the proposed zoning and tracking scheme using a pair of PIR sensors, for simplicity of exposition, installed in an experimental office room whose layout is shown in Figure 2. We shall further discuss one-dimensional zoning, along the horizontal dimension of the room. The coverage areas of the two PIR sensors partially overlap. Thus the detection regions of the sensor have overlapping cells as illustrated in Figure 3. The entire coverage area may be divided into spatial cells that are as large as the cells of the detection region. User presence in a spatial cell results in infrared radiation that in turn corresponds to specific output voltage values at the two PIR sensors.

The output voltage signal at the PIR sensors is first bandpass filtered with cutoff at 0.3 Hz and 8 Hz to remove the continuous signal component and high frequency noise. Denote the resulting signals by $v_k(t)$, $k = 1, 2$. Each signal $v_k(t)$ is quantized using two thresholds, T_{k_1} and T_{k_2}, to characterize nearby and far away areas. The quantization is performed according to the equation:

$$a_k(t) = \begin{cases} 0 & \text{if} \quad -T_{k_1} \le v_k(t) \le T_{k_1}, \\ 0.5 & \text{if} \quad T_{k_1} < v_k(t) \le T_{k_2}, \\ -0.5 & \text{if} \quad -T_{k_2} \le v_k(t) < -T_{k_1}, \\ 1 & \text{if} \quad v_k(t) > T_{k_2}, \\ -1 & \text{if} \quad v_k(t) < -T_{k_2}. \end{cases} \tag{1}$$

Symmetric positive and negative thresholds have been chosen because the PIR analog response is typically symmetric. The thresholds values are set relative to the maximum range learned for each sensor signal, i.e. $T_{k_1} = \alpha_1 M_k$ and $T_{k_2} = \alpha_2 M_k$, where M_k is the 99.9-th percentile of about 15 minutes of signal $v_k(t)$ recorded across several days in an office environment. The parameters α_1 and α_2 can be learned from training data or fixed to values that fit the application.

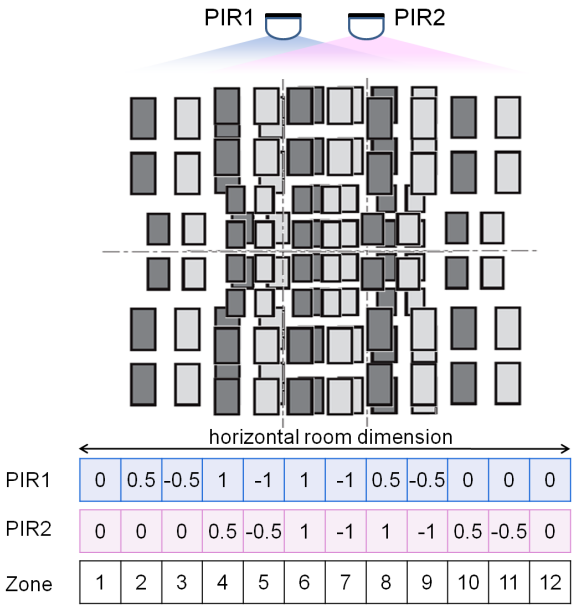

Fig. 3. Overlapping detection regions of the two PIR sensors [top] and spatial encoding of the coverage area depending of the signals' levels [bottom].

For simplicity, here we manually set $\alpha_1 = 0.05$ and $\alpha_2 = 0.5$. We have noticed that slight variations of the parameters can cause minor localization errors, that are typically well recovered by the tracking algorithm.

The key idea is to encode a spatial zone using the quantized signal output $(a_1(t), a_2(t))$. For example, if the signal at PIR1 has a small positive amplitude (thus resulting in $a_1(t) = 0.5$) and the signal from PIR2 is 0 ($a_2(t) = 0$), the user zone is determined to be 2 on the left side of the room. The spatial encoding of the zones over the coverage area is shown in Figure 3. Note that a similar encoding can be obtained for different values of inter-sensor distance, up to a shift of four cells in terms of the corresponding overlap of detection regions.

By matching the expected signal levels from the two sensors with the measured ones, it is possible to localize a target in the coverage area. In practice, this simple approach may incur in errors due to noise, inaccuracies in the thresholding and quantization steps.

These errors can be corrected using tracking. Since the space is discretized here into a number of zones (e.g., 12 zones in the room shown in Figure 3), a natural choice is to identify each zone with a discrete state in a Hidden Markov Model (HMM) [11]. Our HMM $H = (p_{ij}, e_i(a), \pi_i)$ has $N = 12$ hidden Markov states i, $1 \leq i \leq N$ and M possible observables for each state, a, with $1 \leq a \leq M$. The transition probabilities are $p_{ij} = p(q_t = j | q_{t-1} = i)$, with $1 \leq i, j \leq N$ where q_t is the hidden state at time t. The emission probability for the observable a from state i is $e_i(a) =$

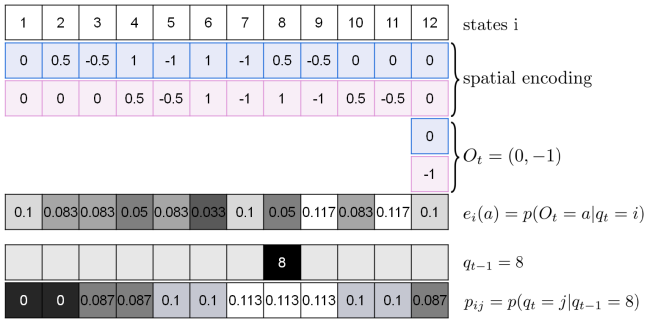

Fig. 4. Derivation of the probabilities $e_i(a)$ and p_{ij} when the observable is $a = (0, -1)$ and the previous state is $q_{t-1} = 8$.

$p(O_t = a | q_t = i)$ where O_t is the observation at time t. The initial state probabilities are $\pi_i = p(q_1 = i)$. Given a sequence of observations $O = O_1, O_2, \ldots, O_t$, and the HMM $H = (p_{ij}, e_i(a), \pi_i)$, our goal is to find the maximum probability state path $Q_t = q_1, q_2, \ldots, q_t$. This can be done recursively using the Viterbi algorithm.

To define the HMM H, the probabilities π_i, p_{ij} and $e_i(a)$ have to be set. We set the initial state probabilities $\pi_i = 1/N$. The transition probabilities p_{ij} are defined as:

$$p_{ij} = \begin{cases} \frac{1}{P}\left(1 - \left\lceil \frac{|i-j|+1}{2} \right\rceil \cdot 0.1\right) & \text{if} \quad |i-j| < 6, \\ 0 & \text{if} \quad |i-j| \geq 6, \end{cases} \tag{2}$$

where P is a normalizing constant that makes p_{ij} a probability. Thus, the probability of transition to closer zones is higher than for zones far away, and it is zero for zones further than five steps.

The emission probabilities $e_i(a)$ reflect the similarity between the observed signal values and the spatial encoding of the coverage area. Each observable, a, is a pair of quantized signals from the two PIR sensors, i.e. $a = (a_1, a_2)$, with $a_k \in \{-1, -0.5, 0, 0.5, 1\}$, $k = 1, 2$. For each state $i = 1, \ldots, 12$ we define a spatial encoding c_i, shown in Figure 3, that associates to each zone a pair of quantized signal values. Let us define the distance between an observed couple of values a and a code c_i, corresponding to a state i, as $d(a, c_i) = 1/4 \cdot (|a_1 - c_i(1)| + |a_2 - c_i(2)|)$. Note that $0 \leq d(a, c_i) \leq 1$. Using the distance d, $e_i(a)$ is defined as

$$e_i(a) = \frac{1}{E} \cdot (1 - d(C_i, a)) \ , \tag{3}$$

where E is a normalizing constant that makes $e_i(a)$ a probability. Figure 4 shows an example of the computation of $e_i(a)$ and p_{ij}.

Let us denote the user zone at time t with x_t. At every time step t, the Viterbi algorithm recovers Q_t, the most probable state path through the model H given the observations available until t. At every time t, the user zone is found as the state q_t of the optimal path Q_t. An outlier detection strategy is

also used to guarantee a certain path continuity. The one proposed here is inspired by classic statistical test approaches [2]. At each step, the target position x_t is determined as:

$$x_t = \begin{cases} q_t & \text{if} \quad |q_t - x_{t-1}| \leq 2A_t^w, \\ \langle q_t, W_t \rangle & \text{if} \quad 2A_t^w < |q_t - x_{t-1}| \leq 6A_t^w, \\ x_{t-1} & \text{if} \quad |q_t - x_{t-1}| > 6A_t^w, \end{cases} \quad (4)$$

where A_t^w is the *average absolute deviation* (AAD) of the w previously selected target locations $W_t = \{x_{t-w}, \ldots, x_{t-1}\}$. Here we set $w = 5$. $\langle q_t, W_t \rangle$ computes the average value of the $w+1$ positions q_t and W_t. If the distance between q_t and the previous target position is small (less than two times the AAD of the last w samples), the estimation q_t is considered valid and assigned to x_t. If the distance is large (more than six times the AAD of the last w samples), q_t is considered an outlier and discarded: x_t is set to the previous value x_{t-1}. In intermediate cases a conservative approach is used where the target x_t is localized in the average position of the last $w+1$ positions q_t and W_t. We term this zoning and tracking method *online Viterbi* tracking.

4. EXPERIMENTAL RESULTS

In this section, we evaluate the performance of the online Viterbi tracker for 1-D zoning and tracking. We also consider two other approaches for comparison. One is final state Viterbi tracking where user zones are determined based on off-line processing of an entire data set. The other method is binary localization based on processing the PIR binary decision outputs. In this method, when both PIR sensors trigger a detection, the target is localized in the center of the room (zones 4 to 9), while if only one PIR detector triggers a detection, the target is localized on the corresponding side of the room (zones 2, 3 or 10, 11). If no detection is triggered, the target is out of the coverage area (zones 1 or 12). For fairness of comparison, the detection threshold for each PIR is chosen to be T_{k_1}.

To evaluate the proposed approaches, we recorded the PIR output voltages while a person was walking in the room in different trajectories. The voltage signals are sampled at 10 kHz, band-pass filtered between 0.3 Hz and 8 Hz and quantized using (1). The quantized signals are then downsampled at 10 Hz by keeping the mode (i.e. the most frequent value) of the signals over non-overlapping windows of 1000 samples. User zones are determined every 100 ms for the binary localization and online Viterbi methods.

Figure 5 shows the results for the three zoning and tracking methods. Four recordings, each of duration over 20 seconds corresponding to 200 points, were made. In (a) a person walks from left to right and back two times and then stops under PIR1 for few seconds, as depicted on the top row of the picture. In (b) a person walks perpendicular to the sensors. This scenario is challenging because the sensor sensitivity in the perpendicular direction is lower. Therefore, if a person walks perpendicular to the sensors, the PIR output voltage is lower. In (c) a person walks around the room two times. In (d) a person crosses the room twice. The approximate trajectories followed by the target are sketched on top of each plot. The gray area shows the zoning result using binary localization, the blue circles indicate the user zone estimated using the online Viterbi tracker, and the most probable state path found with the final state Viterbi algorithm knowing all the data points, Q_{200}, is plotted with red crosses.

In the simple case in (a), the binary localization approach can provide coarse user zoning in the coverage area, while the online Viterbi method provides accurate zoning and tracking. However, in the most challenging scenarios shown in Figures 5 (b), (c) and (d), the binary zoning method incurs many errors. In these scenarios, the performance advantage of the Viterbi tracking method is clear. Note that the final state Viterbi tracking results in a few errors largely due to outliers not being filtered out as done in the online Viterbi tracking algorithm.

5. CONCLUSIONS

We presented a method for indoor user zoning and tracking with a PIR sensing system located in the ceiling. The paper demonstrates how statio-temporal processing of raw output voltages from PIR sensors can provide finer user localization and improved tracking accuracy in PIR sensor systems. The performance of the method was shown using commercial PIR sensors in an experimental setup. The proposed method can be extended to 2-D zoning using quad-type PIR sensors [9]. Future work will also extend the developed method to multi-user zoning and tracking.

6. REFERENCES

[1] Y. Agarwal, B. Balaji, S. Dutta, R. K. Gupta and T. Weng, "Duty-cycling buildings aggressively: The next frontier in HVAC control", *International Symposium on Information Processing in Sensor Networks*, pp. 246-257, 2011.

[2] V. Barnett and T. Lewis, "Outliers in Statistical Data", *John Wiley and Sons*, 1994.

[3] E. L. Dereniak and G. D. Boreman, "Infrared detectors and systems", Wiley-Interscience, 1996.

[4] P. M. Djuric, M. Vemula and M. F. Bugallo, "Target tracking by particle filtering in binary sensor networks", *IEEE Transactions on Signal Processing*, pp. 2229-2238, 2008.

[5] B. F. La Scala, M. R. Morelande and C.O. Savage, "Robust target tracking with unreliable binary proximity sensors", *International Conference on Acoustics, Speech and Signal Processing*, pp. 953-956, 2006.

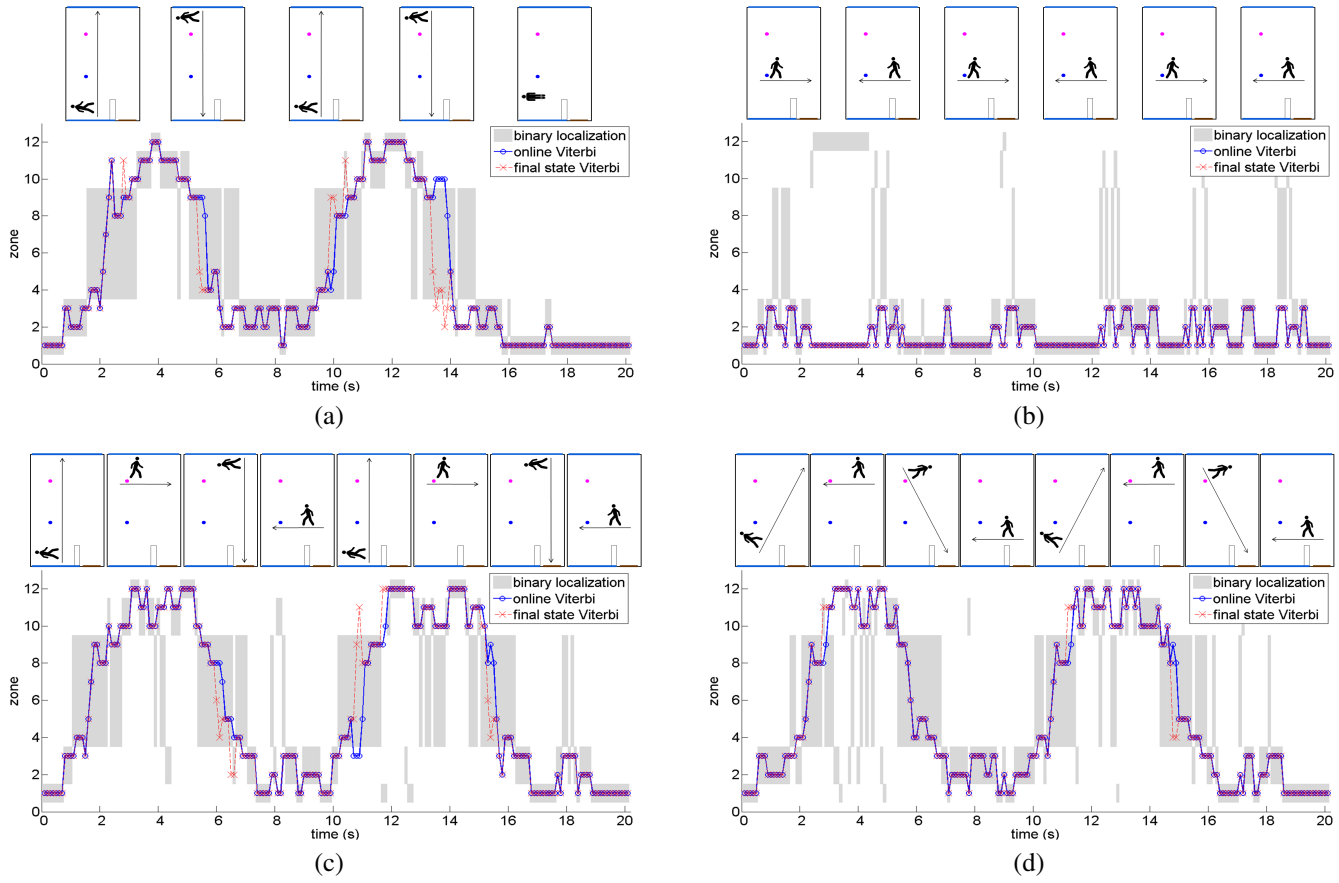

Fig. 5. Zoning and tracking results for the binary localization method (gray area), the online Viterbi tracker (blue circles) and the most probable state path found by the final state Viterbi algorithm knowing all the data points (red crosses). The four experiments show: (a) a person walking from left to right and back two times and then stopping under PIR1; (b) a person walking perpendicular to the sensors; (c) a person walking around the room twice and (d) a person crossing the room twice. The approximate trajectories followed by the target are sketched on top of each plot.

[6] X. Liu, G. Zhao and X. Ma, "Target localization and tracking in noisy binary sensor networks with known spatial topology", *International Conference on Acoustics, Speech and Signal Processing*, pp. 1029-1032, 2007.

[7] Murata manufacturing, "Pyroelectric Infrared Sensors", `http://www.murata.com/products/catalog/pdf/s21e.pdf`.

[8] V. S. Nithya, K. Sheshadri, A. Kumar and K. V. S. Hari, "Model based target tracking in a wireless network of passive infrared sensor nodes", *International Conference on Signal Processing and Communications*, 2010.

[9] Panasonic, "MP Motion Sensor NaPiOn", `http://panasonic-denko.co.jp/ac/e/control/sensor/human/napion/`.

[10] A. Pandharipande and D. Caicedo, "Daylight integrated illumination control of LED systems based on enhanced presence sensing", *Energy and Buildings*, pp. 944-950, 2011.

[11] L. R. Rabiner, "A tutorial on hidden Markov models and selected applications in speech recognition", *Proceedings of the IEEE*, pp. 257-286, 1989.

[12] J. Singh, U. Madhow, R. Kumar, S. Suri and R. Cagley, "Tracking multiple targets using binary proximity sensors", *International Symposium on Information Processing in Sensor Networks*, 2007.

[13] X. Xie and R. J. Evans, "Multiple target tracking and multiple frequency line tracking using hidden Markov models", *IEEE Transactions on Signal Processing*, pp. 2659-2676, 1991.

[14] P. Zappi, E. Farella and L. Benini, "Tracking motion direction and distance with pyroelectric IR sensors", *IEEE Sensors Journal*, pp. 1486-1494, 2010.